Journal of Hydrology 556 (2018) 1050–1063

Contents lists available at ScienceDirect

Journal of Hydrology

journal homepage: www.elsevier.com/locate/jhydrol

Research papers

Impact of air temperature on physically-based maximum precipitation estimation through change in moisture holding capacity of air

K. Ishida [a,*], N. Ohara [b], M.L. Kavvas [a], Z.Q. Chen [c], M.L. Anderson [d]

[a] Hydrologic Research Laboratory, Department of Civil and Environmental Engineering, University of California, Davis, One Shields Avenue, Davis, CA 95616, USA
[b] Department of Civil and Architectural Engineering, University of Wyoming, 1000 E. University Avenue, Laramie, WY 82071, USA
[c] Bay Delta Office, California Department of Water Resources, 1416 Ninth Street, Sacramento, CA 95814, USA
[d] Hydrology and Flood Operations Office, California Department of Water Resources, 3310 El Camino Avenue, Sacramento, CA 95821, USA

ARTICLE INFO

Article history:
Available online 6 October 2016

Keywords:
Probable Maximum Precipitation (PMP)
Regional atmospheric model
Dynamical downscaling
Climate change
Hydraulic structure design
Atmospheric river

ABSTRACT

Impact of air temperature on the Maximum Precipitation (MP) estimation through change in moisture holding capacity of air was investigated. A series of previous studies have estimated the MP of 72-h basin-average precipitation over the American River watershed (ARW) in Northern California by means of the Maximum Precipitation (MP) estimation approach, which utilizes a physically-based regional atmospheric model. For the MP estimation, they have selected 61 severe storm events for the ARW, and have maximized them by means of the atmospheric boundary condition shifting (ABCS) and relative humidity maximization (RHM) methods. This study conducted two types of numerical experiments in addition to the MP estimation by the previous studies. First, the air temperature on the entire lateral boundaries of the outer model domain was increased uniformly by 0.0–8.0 °C with 0.5 °C increments for the two severest maximized historical storm events in addition to application of the ABCS + RHM method to investigate the sensitivity of the basin-average precipitation over the ARW to air temperature rise. In this investigation, a monotonous increase was found in the maximum 72-h basin-average precipitation over the ARW with air temperature rise for both of the storm events. The second numerical experiment used specific amounts of air temperature rise that is assumed to happen under future climate change conditions. Air temperature was increased by those specified amounts uniformly on the entire lateral boundaries in addition to application of the ABCS + RHM method to investigate the impact of air temperature on the MP estimate over the ARW under changing climate. The results in the second numerical experiment show that temperature increases in the future climate may amplify the MP estimate over the ARW. The MP estimate may increase by 14.6% in the middle of the 21st century and by 27.3% in the end of the 21st century compared to the historical period.

© 2016 Elsevier B.V. All rights reserved.

1. Introduction

Estimates of the extreme flood discharges are required to design large hydraulic structures, such as dams and flood protection structures. In hydraulic structure design, the extreme flood discharge is supposed to be the physical upper bound of flow discharge at the drainage area of the targeted hydraulic structure, namely at the targeted watershed. However, it is not simple to obtain the "physical" upper bound of flow discharge due to the non-linearity and complexity of its physical mechanisms. Streamflow is a component of hydrological processes, but it is also influenced by atmospheric phenomena. Especially, precipitation is a major input of water from atmospheric processes to hydrological processes, and frequently dominates the amount of flow discharge at a watershed. Therefore, understanding of physical mechanisms of the extreme precipitation is necessary to estimate the extreme flood discharge at a targeted watershed. In other words, estimating the physical upper bound of precipitation over a targeted watershed with consideration of its physical mechanisms will be the first step for the extreme flood estimation.

The probable maximum precipitation (PMP) approach has been widely used to estimate the extreme precipitation (e.g. Casas et al., 2011; Corrigan et al., 1999; Fernando and Wickramasuriya, 2011; Kulkarni et al., 2010; U.S. Weather Bureau, 1961, 1966; Zhan and Zhou, 1984), which was achieved by collaborative efforts among hydrologists and meteorologists since the middle of 1930s (Stallings et al., 1986). According to World Meteorological

* Corresponding author.
E-mail addresses: kishida@ucdavis.edu (K. Ishida), nohara1@uwyo.edu (N. Ohara), mlkavvas@ucdavis.edu (M.L. Kavvas), zchen@water.ca.gov (Z.Q. Chen), michael.l.anderson@water.ca.gov (M.L. Anderson).

http://dx.doi.org/10.1016/j.jhydrol.2016.10.008
0022-1694/© 2016 Elsevier B.V. All rights reserved.

Organization (WMO) (1986), PMP is defined as the meteorologically possible upper bound of precipitation over a targeted size of storm area at a particular location at a certain time of the year without long-term climatic trend. The PMP approach basically utilizes observed precipitation, and maximizes precipitation based on the observed values by means of simple physical relationships between precipitation and other observable variables such as dew-point temperature and wind speed. Despite many applications, however, there are some fundamental issues on the PMP approach. PMP estimates are excessively sensitive to availability of the observation data (Papalexiou and Koutsoyiannis, 2006). A simple physical relationship between precipitation and other variables may be unable to describe complicated precipitation mechanisms (Abbs, 1999). Although the traditional PMP approach has been very useful as a tool for hydraulic structure design, it was originally developed many decades ago when computational resources were considerably limited.

The dynamical downscaling technique with a physically-based atmospheric model is nowadays a useful tool not only in atmospheric science, but also in hydrological engineering. Although the dynamical downscaling technique requires large computational resources, recent development in the information technology has enabled the dynamical downscaling technique to be applied to various hydrological problems (e.g., Kavvas et al., 2013; Kay et al., 2006; Kure et al., 2013; Markus et al., 2011; Trinh et al., 2016; Yoshitani et al., 2009). For the estimation of maximum precipitation over a watershed an approach has recently been developed based on the dynamical downscaling technique to estimate the physical upper bound of precipitation over the targeted watershed by means of a physically-based regional atmospheric model (Ishida et al., 2015a, 2015b; Ohara et al., 2011). This approach first investigates storm systems that caused severe precipitation over the targeted watershed. After selecting a sufficient number of severe storm events through the investigation of the historical storm systems, this approach maximizes precipitation over the targeted watershed for each of the selected storm events with respect to their physical mechanisms by means of a regional atmospheric model. Then the largest value of precipitation among the maximized results for all the storm events is considered as the upper bound of precipitation over the targeted watershed. The physical upper bound of precipitation estimated by this approach is referred to as Maximum Precipitation (MP) to differentiate it from the aforementioned traditional PMP. Accordingly, this fully physically-based approach is called the MP estimation approach, or the physically-based PMP (PhysPMP) approach as an alternative to the widely-known traditional PMP approach. Due to the use of a regional atmospheric model, the MP estimation approach requires no observations except for those limited observations that are necessary for the calibration and validation of the regional atmospheric model.

Like the traditional PMP approach, the MP estimation approach also requires methods to maximize precipitation over a targeted watershed. After the preliminary study of Ohara et al. (2011), Ishida et al. (2015a, 2015b) developed two methods with a regional atmospheric model to maximize the contribution of storm systems to precipitation over a targeted watershed. First, the path of a storm system during a selected storm event is optimized by shifting the atmospheric boundary conditions of the regional atmospheric model over the target watershed in space with respect to latitude and longitude in order to maximize the contribution of the storm system to precipitation over the target watershed. After the optimization of the path of the storm system, the moisture of the storm system is maximized by setting relative humidity on the boundaries of the regional atmospheric model at 100% in order to maximize the potential of the storm system with respect to moisture. The former method is called the atmospheric boundary condition shifting (ABCS) method, and the latter is the relative humidity maximization (RHM) method. When the RHM method is applied together with the ABCS method, the combined method is referred to as the ABCS + RHM method in this paper.

The ABCS method and the RHM method may be essential for the MP estimation approach because the path and moisture of a storm system have significant effects on the precipitation depth over the targeted watershed. Meanwhile, other atmospheric variables may also influence precipitation depth. Especially, air temperature may be of great interest because global warming is a major aspect of climate change. According to an analysis on future climate projection data by Kunkel et al. (2013), the magnitudes of the maximum precipitable water will increase with air temperature rise, magnifying the extreme precipitation in the future.

In this context, this study focuses on air temperature among various atmospheric variables, and investigates its impact on the MP estimation through change in moisture holding capacity of air. As the target watershed, the American River watershed (ARW) in Northern California is selected. It is one of the three target watersheds in the previous MP estimation studies by Ishida et al. (2015a, 2015b). Two types of numerical experiments will be conducted to investigate the impact of air temperature on the MP estimate of 72-h basin-average precipitation over the ARW that was obtained by the ABCS + RHM method in the previous studies (Ishida et al., 2015a, 2015b). First, the air temperature on the entire lateral boundaries of the domains of a regional atmospheric model will be gradually increased uniformly along the lateral boundaries in addition to the application of the ABCS + RHM method in order to investigate the influence of air temperature on the MP estimate through increase in the moisture holding capacity of air over the ARW. Secondly, the air temperature will be raised to some specific values that are assumed to represent future conditions under changing climate. Since air temperature is a major indicator of climate change, the second numerical experiment is assumed to result in the MP estimate over the ARW under future climate change conditions.

2. Methodology

This study investigates the impact of air temperature on the MP estimate through change in the moisture holding capacity of air by several numerical experiments. For the numerical experiments, air temperature is raised uniformly at the entire lateral boundaries of the outer model domain of a regional atmospheric model to increase the moisture holding capacity of a storm system that brings moisture from the outside of the outer model domain to the targeted watershed. This method is referred to as the air temperature adjustment (ATA) method. It is noted that all the methods for the MP estimation should be applied only to the boundaries of the outer model domain except at the initial state in order to conserve mass, momentum, and energy within the model domains during the simulation.

In this study, numerical experiments with the ATA method were conducted in addition to the MP estimation by the ABCS + RHM method of the previous studies (Ishida et al., 2015a, 2015b). Since air temperature rise expands the capacity of moisture in the air, air temperature is an important factor that influences precipitation depth. If the air contains more moisture, a storm system may be able to produce heavier precipitation. However, air temperature rise alone does not increase the amount of moisture in the air, and may reduce relative humidity. Less relative humidity may cause less precipitation. To magnify precipitation depth by the ATA method, therefore, relative humidity has to be taken into account. As such, it is recommended that the ATA method is utilized together with the RHM method for the MP

estimation. This combined use of the ATA method and the RHM method raises air temperature while keeping relative humidity at 100% on the entire model lateral boundaries, which results in increase in the air moisture on the model boundaries. Consequently, this combined use increases the moisture of atmospheric flows at synoptic scale that come from the outside into the outer model regional-scale domain during the model simulation. As explained in Ishida et al. (2015b) in detail, the RHM method is run together with the ABCS method in MP estimation so that the impact of the RHM method can be concentrated on enhancing the contribution of a specific storm system to precipitation over a targeted watershed. In the same manner, the ATA method with the RHM method is also applied together with the ABCS method to increase the moisture of a specific storm system that historically caused severe precipitation over the target watershed.

3. Targeted watershed and model configuration

The ARW is located over the west slope of Sierra-Nevada Mountain range in Northern California in the United States (Fig. 1). There is a large reservoir at the outlet of the ARW, which is called Folsom Lake. Folsom Lake is formed by Folsom dam. Folsom dam plays an important role in flood protection because it is located at just upstream of Sacramento, the capital city of California.

This study utilizes the same regional atmospheric model, the same configuration of the regional atmospheric model, and the same global atmospheric data for its original initial and boundary conditions in the previous MP estimation studies of Ishida et al. (2015a, 2015b), which were calibrated and validated in Ohara et al. (2011) and Ishida et al. (2015a) by comparing the model simulations under various configurations with the corresponding observation data. The selected regional atmospheric model is the fifth generation Penn State/National Center for Atmospheric Research (NCAR) Mesoscale Model (MM5; Grell et al., 1994). Fig. 2 shows the four nested domains for the MM5. The four nested domains consist of 24 × 22 horizontal grid points at 81 km resolution, 37 × 31 horizontal grid points at 27 km resolution, 73 × 49 horizontal grid points at 9 km resolution, and 175 × 109 horizontal grid points at 3 km resolution, respectively, with 24 vertical levels. The MM5 was configured with the following model options; Kain-Fritsch 2 scheme (Kain and Fritsch, 1993) for the cumulus

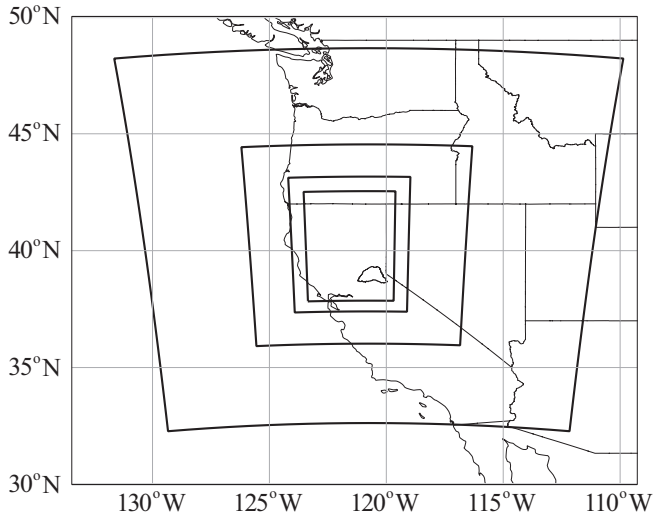

Fig. 2. Nested model domains.

parameterization, Reisner graupel scheme (Reisner et al., 1998) for the microphysics processes, medium-range forecast scheme (Hong and Pan, 1996) for the planetary boundary layer processes, the cloud-radiation scheme (NCAR, 2005) for a radiation processes, and five-layer soil model (Dudhia, 1996) for the land surface processes. The MP estimation approach with a regional atmospheric model requires global atmospheric data for the model's initial and boundary conditions, which are to be adjusted by the aforementioned methods. As the global atmospheric data, NCAR/National Centers for Environmental Prediction (NCEP) Reanalysis I dataset (Kalnay et al., 1996) was employed.

4. Application

The MP estimation approach requires severe storm events over a targeted watershed to maximize precipitation over the watershed. Ishida et al. (2015a) selected 61 severe storm events for the ARW from 61 water years from October 1, 1950 through

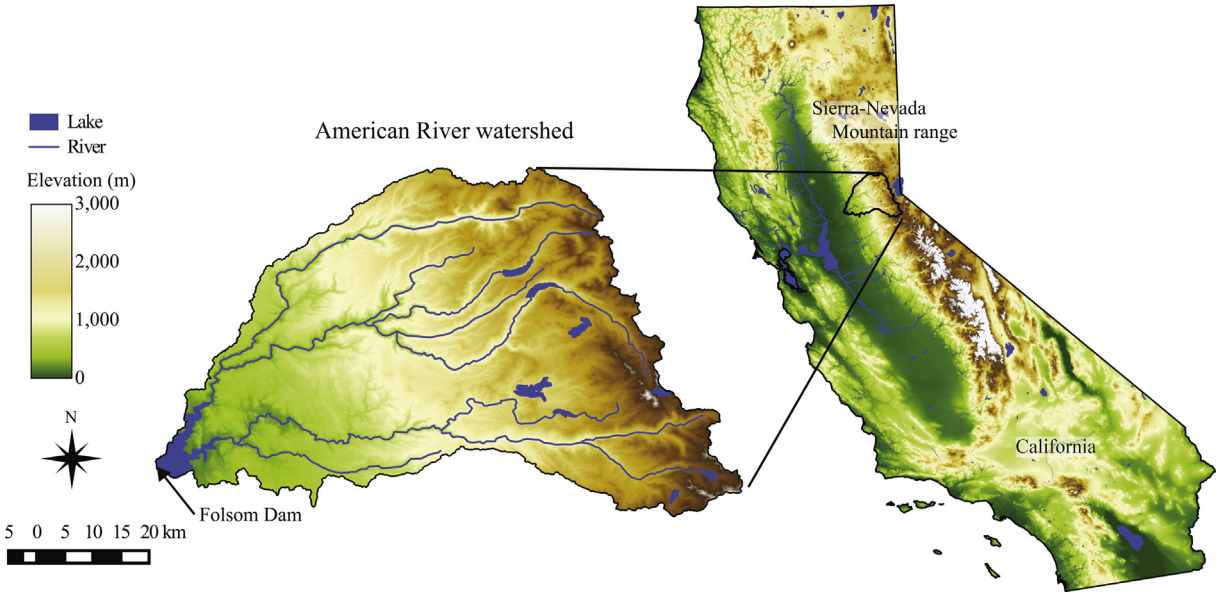

Fig. 1. Plan view of the targeted watershed.

September 30, 2011, based on the simulation of precipitation fields over ARW during this historical period. The selected storm events are shown in Table 1. The name of the storm events consists of the letter "A" of the ARW, two digits of the year, and two digits of the months of the storm events. When there are more than two storm events in the same month of the same year, the storm event names are differentiated by a suffix. These 61 selected severe storm events for the ARW in the previous studies were also used in this study.

Severe precipitation is mostly caused by a high-moisture synoptic-scale atmospheric flow, the so-called "atmospheric river (AR)" in Northern California where the ARW is located. Ishida et al. (2015a) focused on 72-h basin-average precipitation because 72-h precipitation or 72-h flood discharge is generally used for hydraulic structure design in California. Then, they shifted the atmospheric river to the optimal path to maximize the 72-h basin-average precipitation over the ARW for each of the 61 selected storm events by the ABCS (Atmospheric Boundary Condition Shifting) method. After the application of the ABCS method, Ishida et al. (2015b) utilized the RHM (Relative Humidity Maximization) method to maximize the moisture of the atmospheric river.

In addition to the ABCS + RHM method, this study applies the ATA (Atmospheric Temperature Adjustment) method to the selected storm events for the ARW by means of the MM5 with the aforementioned configuration in order to investigate the impact of air temperature on the MP estimate over the ARW. The ATA method together with the RHM method will provide more moisture than by the RHM method alone, for the atmospheric rivers that strike the ARW by the ABCS method.

The ATA method in addition to the ABCS + RHM method is first applied to two of the 61 selected severe storm events; the A9701a and the A9501 storm events. Air temperature on the boundaries is increased uniformly by 0.0 °C to 8.0 °C with 0.5 °C intervals by the ATA method in addition to the ABCS + RHM method in order to investigate the sensitivity of basin-average precipitation over the ARW to air temperature rise. For simplification, each case of the numerical experiments is referred to as ATA with a specific increase in air temperature. For example, ATA2.5 means that air temperature on the entire lateral boundaries is increased by 2.5 °C uniformly by the ATA method in addition to the ABCS + RHM method, while ATA0.0 means a case that uses only the ABCS + RHM method. The A9701a storm event is one of the most severe historical storm events, and the second largest storm event by the ABCS + RHM method (Ishida et al., 2015b). The period of the A9701a storm event is from December 26, 1996 through January 6, 1997. Fig. 3 shows the precipitable water over the Pacific Ocean at 6:00 h on January 1, 1997. A large atmospheric river that was originally a remnant of a tropical cyclone came from the west sector of the Pacific Ocean. Another large atmospheric river came from the middle sector of the tropical zone of the Pacific Ocean. Those two large atmospheric rivers merged together over the Pacific Ocean, and became a single huge atmospheric river before it hit the west coast of the United States. The A9501 storm event produced the largest storm event with respect to basin-average precipitation after application of the ABCS + RHM method (Ishida et al., 2015b). The A9501 storm event started on January 4, 1995, and ended on January 18, 1995. The atmospheric river of the A9501 storm event was narrow compared to that of the A9701a storm event as illustrated in Fig. 4 although the atmospheric river of the A9501 storm event historically caused intense precipitation over some parts of Northern California.

Secondly, the ATA method in addition to the ABCS + RHM method is applied to all the 61 selected storm events to investigate the impact of air temperature on the MP estimate over the ARW under changing climate. Jang et al. (2012) assessed future climate change effects on air temperature in Northern California based on future climate projections. That climate change assessment study states that air temperature will increase by 1.36 °C by water year 2055 and by 3.16 °C by water year 2099 over the ARW compared to water year 2010. The amount of air temperature rise that was estimated in that climate change assessment study is for the inner model domain and not on the boundaries of the outer model domain, and is not based on the air temperature during each storm event. However, the magnitude of air temperature rise over the ARW in that future climate change study may be informative for the investigation of the impact of air temperature rise on the MP estimate under changing climate. Therefore, in this study the air temperature is increased uniformly by 1.36 °C and 3.16 °C on the entire lateral boundaries of the outer domain for the 61 selected severe storm events by the ATA method in addition to the ABCS + RHM method during numerical experiments for the estimation of the maximum 72-h basin-average precipitation over ARW.

Table 1
Periods of the 61 selected severe storm events over the American River watershed (Ishida et al., 2015a).

Event	Period	Event	Periods
A5011	11/14/1950–11/24/1950	A8202	02/14/1982–02/19/1982
A5201	01/07/1952–01/19/1952	A8204a	03/26/1982–04/09/1982
A5402	02/12/1954–02/21/1954	A8204b	04/10/1982–04/17/1982
A5512	12/17/1955–12/30/1955	A8303	02/25/1983–03/05/1983
A5702	02/21/1957–03/08/1957	A8403	03/13/1984–03/20/1984
A5804	03/29/1958–04/09/1958	A8602	02/12/1986–02/23/1986
A5902	02/15/1959–02/24/1959	A8603	03/07/1986–03/19/1986
A6002	02/01/1960–02/13/1960	A8811	11/22/1988–11/28/1988
A6202	02/07/1962–02/23/1962	A9103	03/01/1991–03/08/1991
A6210	10/11/1962–10/17/1962	A9212	12/28/1992–01/04/1993
A6302	01/30/1963–02/06/1963	A9301a	01/06/1993–01/19/1993
A6412	12/19/1964–01/10/1965	A9301b	01/20/1993–01/25/1993
A6512	12/24/1965–01/08/1966	A9501	01/04/1995–01/18/1995
A6701	01/20/1967–02/03/1967	A9503a	03/09/1995–03/18/1995
A6703	03/10/1967–03/20/1967	A9503b	03/20/1995–03/26/1995
A6801	01/27/1968–02/03/1968	A9512	12/11/1995–12/18/1995
A6901a	01/12/1969–01/17/1969	A9602	02/18/1996–03/03/1996
A6901b	01/19/1969–02/02/1969	A9611	11/17/1996–11/25/1996
A6902	02/12/1969–03/06/1969	A9612	12/05/1996–12/15/1996
A6912	12/19/1969–12/28/1969	A9701a	12/26/1996–01/06/1997
A7311	11/05/1973–11/25/1973	A9701b	01/20/1997–01/29/1997
A7403a	02/27/1974–03/06/1974	A9902	02/06/1999–02/12/1999
A7403b	03/27/1974–04/04/1974	A0002	02/10/2000–02/19/2000
A7502	01/31/1975–02/16/1975	A0211	11/07/2002–11/12/2002
A7801	01/03/1978–01/22/1978	A0212	12/13/2002–12/24/2002
A7802	02/05/1978–02/16/1978	A0303	03/14/2003–03/20/2003
A7803	03/01/1978–03/08/1978	A0601	12/18/2005–01/06/2006
A8001	01/09/1980–01/20/1980	A0801	01/03/2008–01/12/2008
A8002	02/14/1980–02/26/1980	A0903	03/01/2009–03/07/2009
A8101	01/23/1981–02/02/1981	A1001	01/17/2010–01/29/2010
A8111	11/13/1981–11/20/1981		

5. Results and discussion

5.1. Sensitivity of MP estimate to air temperature

Fig. 5 shows the amplified maximum 72-h basin-average precipitation over the ARW during the A9701a and the A9501 storm events by increasing the air temperature uniformly on the entire boundaries of the outer domain with the ATA method in addition to the ABCS + RHM method. The peak of the 72-h basin-average precipitation increases over the ARW for both of the storm events by the rise in air temperature. The MP estimate of the 72-h basin-average precipitation over the ARW by the ABCS + RHM method (ATA0.0) was 686 mm for the A9701a storm event (Ishida et al., 2015b). The MP estimate by the original ABSC + RHM approach increases to 798 mm by the additional ATA2.0, 935 mm by the

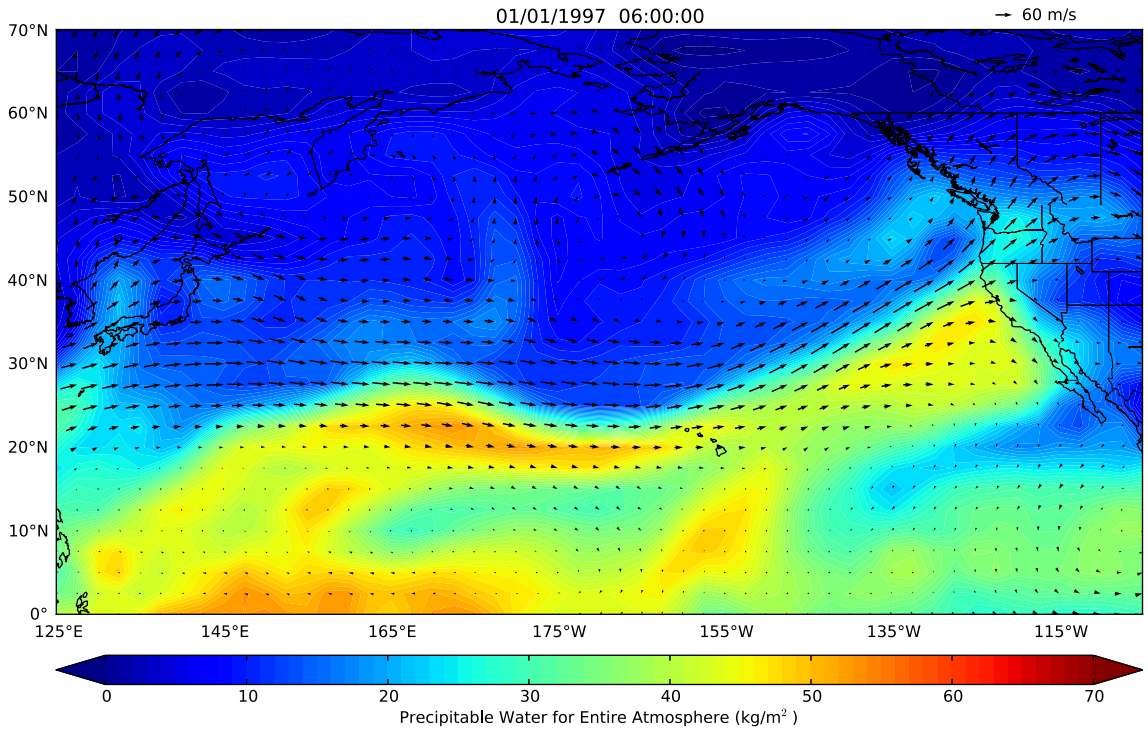

Fig. 3. Precipitable water together with the wind fields at the 300 hPa level over Pacific Ocean at 6:00 h on January 1, 1997 based on the NCAR/NCEP Reanalysis I data.

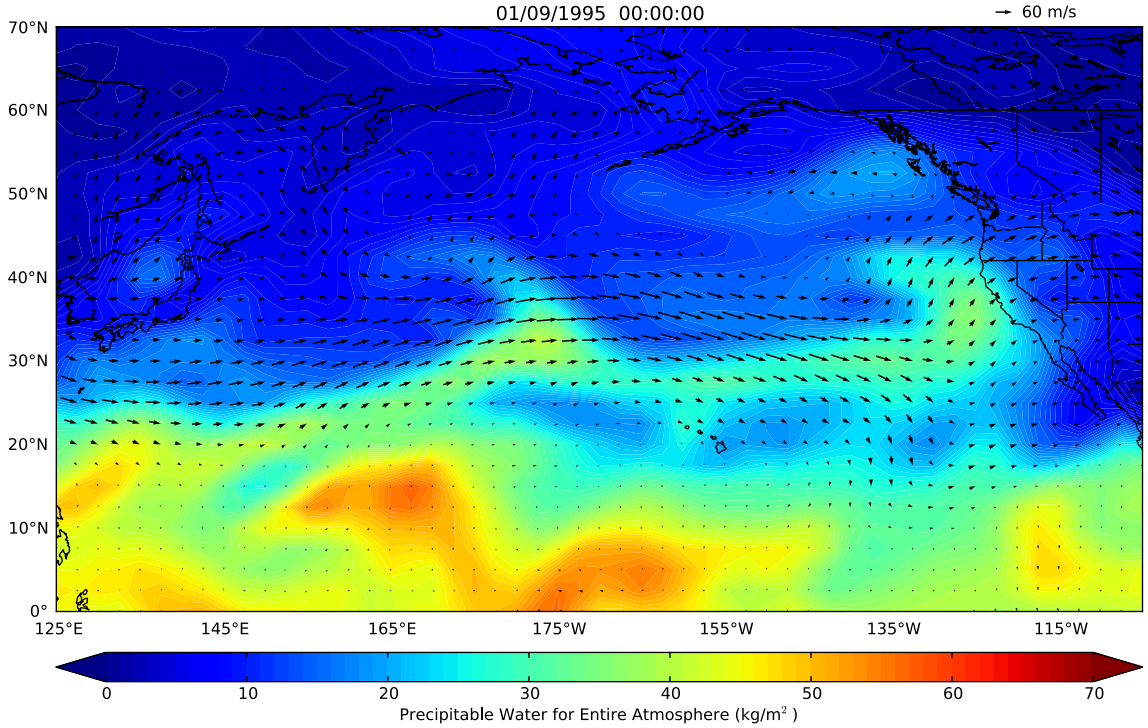

Fig. 4. Precipitable water together with the wind fields at the 300 hPa level over Pacific Ocean at 0:00 h on January 9, 1995 based on the NCAR/NCEP Reanalysis I data.

additional ATA4.0, 1056 mm by the additional ATA6.0, and 1199 mm by the additional ATA8.0. The percentage increases in the MP estimate are 16.5%, 36.5%, 54.1%, and 74.9% respectively, compared to the result by ATA0.0. The MP estimate by the ABCS + RHM method (ATA0.0) was 738 mm for the A9501 storm event (Ishida et al., 2015b). The MP estimate by the original ABSC + RHM approach increases to 878 mm by the additional ATA2.0, 929 mm by the additional ATA4.0, 1055 mm by the additional ATA6.0, and 1330 mm by the additional ATA8.0. The percentage increases from the results of ATA0.0 are 18.9%, 25.9%, 42.9%, and 80.2%, respectively. The 72-h basin-average precipitation increases almost linearly for the A9701a storm event by the additional ATA method whereas there are some perturbations on the results for the A9501 storm event.

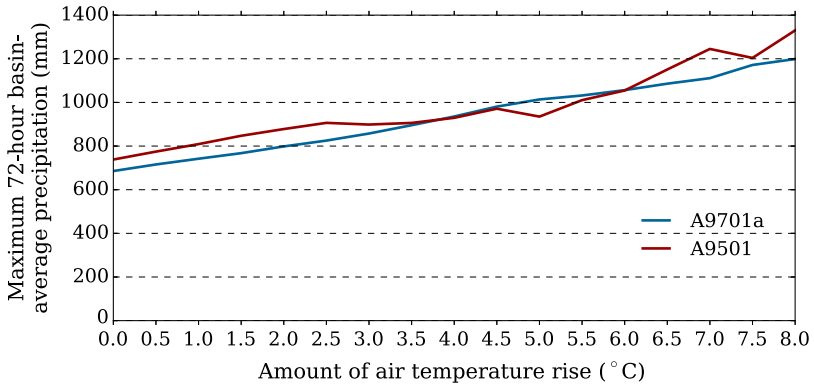

Fig. 5. Change in maximum 72-h basin-average precipitation over the ARW with air temperature rise uniformly on the boundaries of the outer model domain for the A9701a and the A9501 storm events.

Fig. 6 shows the hourly basin-average precipitation and its 72-h moving summation for the amplified results over the ARW for the A9701a storm event by the ATA method in addition to the ABCS + RHM method. Hourly basin-average precipitation increases monotonously during each peak over the ARW as air temperature rises on the entire lateral boundaries uniformly. As a consequence of the increase of the hourly basin-average precipitation during each peak, the 72-h moving summation in basin-average precipitation is also amplified. Fig. 7 shows the precipitation fields within the inner model domain during the 72-h period when the maximum 72-h basin-average precipitation occurs over the ARW for each temperature rise case for the A9701a storm event. Precipitation gradually increases over almost all the inner model domain with air temperature rise. Since the atmospheric river in the A9701a storm event was huge, the ATA method amplifies the water vapor flux over a wide area as shown in Fig. 8. This amplification of water vapor flux causes heavier precipitation over a wide area. Meanwhile, precipitation is amplified especially over the ARW by the ATA method. This concentrated amplification of precipitation over the ARW is probably because the path of the atmospheric river was already optimized by the ABCS method.

Fig. 9 shows the hourly basin-average precipitation and its 72-h moving summation over the ARW for the A9501 storm event by the ATA method in addition to the ABCS + RHM method. Hourly basin-average precipitation increases mainly during the two original largest peaks from 0:00 h on January 9, 1995 to 12:00 h on January 10, 1995 over the ARW. Especially, the first peak at 10:00 h on January 9, 1995 is significantly amplified by the ATA method. The increase in the two peaks of hourly basin-average precipitation in turn increases the maximum 72-h basin-average precipitation over the ARW for the A9501 storm event. Fig. 10 shows the precipitation fields within the inner model domain and the time-averaged wind fields at the 500 hPa pressure level during the 72-h period during which the maximum 72-h basin-average precipitation occurs over the ARW for each of the temperature rise cases for the A9501 storm event. Unlike the A9701a storm event, precipitation is amplified only around the ARW by the additional ATA method. As illustrated in Fig. 11, the additional ATA method intensifies only the high-moisture atmospheric flow toward the ARW. Meanwhile, the precipitation fields slightly but gradually shift toward southeast as air temperature increases on the boundaries of the model domain. This shift in the precipitation field is caused by a small change in the wind direction with air temperature rise although this small change in the wind direction is difficult to detect in Fig. 10. In addition to the narrowness of the high-moisture atmospheric flow, this shift in the direction of the precipitation fields causes the changes in the maximum 72-h basin-average precipitation for the A9501 storm event shown in Fig. 5.

While all the peaks of hourly basin-average precipitation for the A9701a storm event are amplified by the additional ATA method (Fig. 6), some small peaks for the A9501 storm event are not influenced by the additional ATA method (Fig. 9). For example, the peak

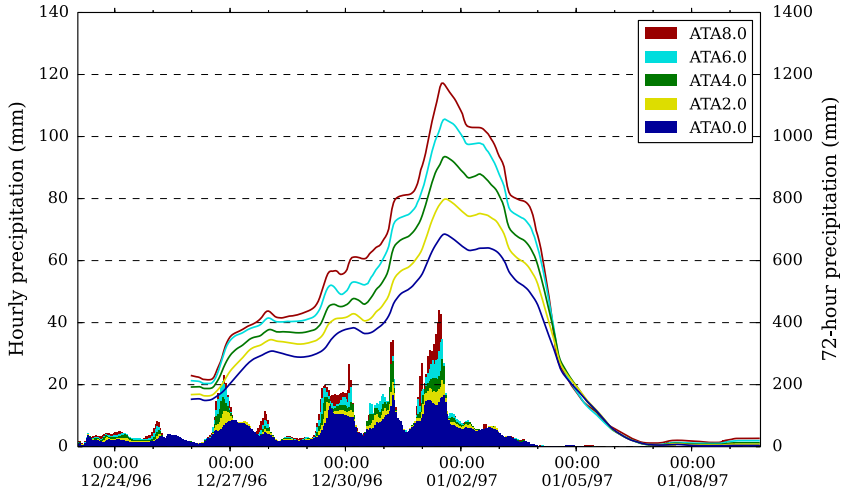

Fig. 6. Hourly basin-average precipitation (bar) and its 72-h moving summation (line) over the ARW for the A9701a storm event for ATA0.0 (only ABCS + RHM), ATA2.0, ATA4.0, ATA6.0, and ATA8.0.

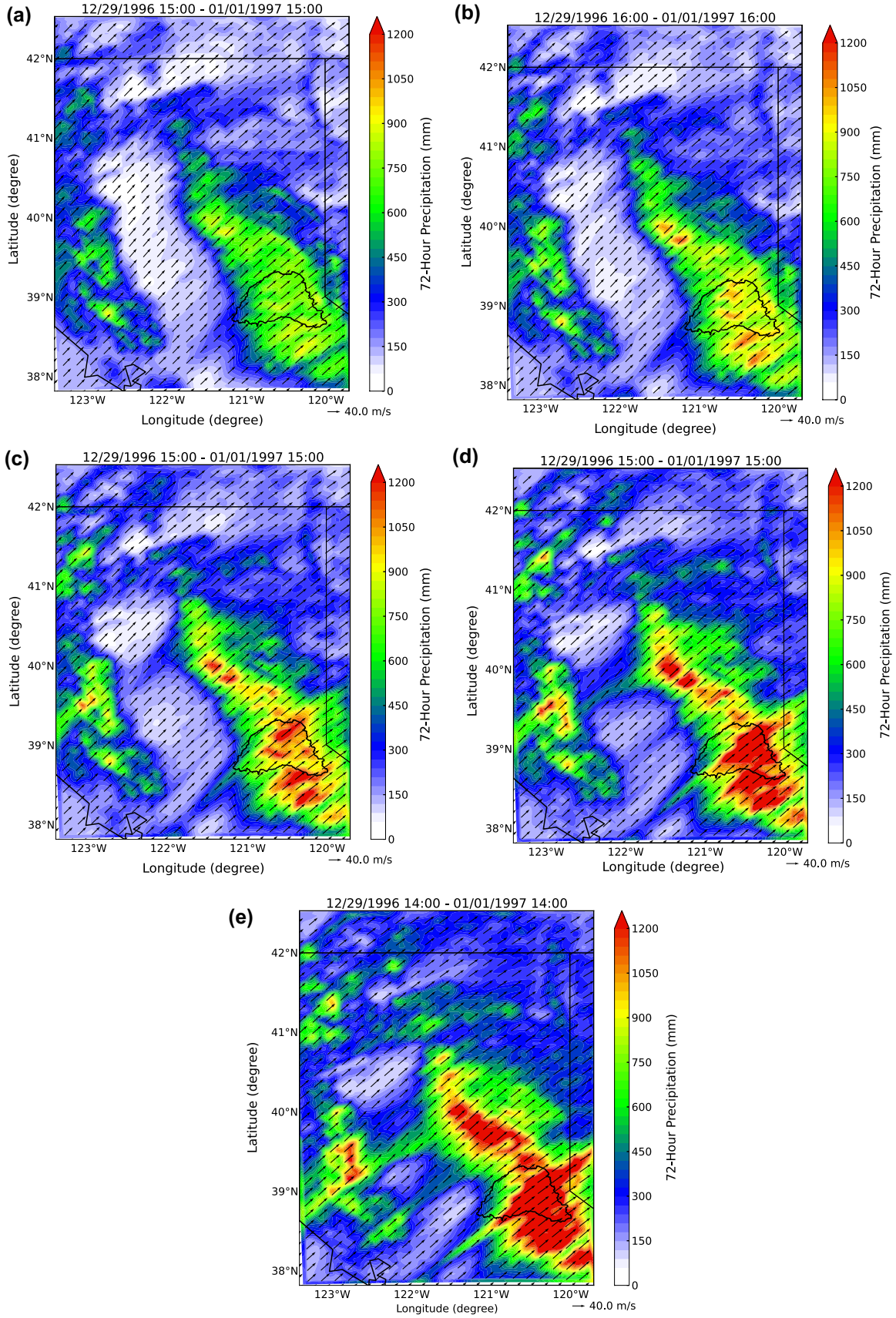

Fig. 7. 72-h precipitation depth for the A9701a storm event by (a) ATA0.0 (only ABCS + RHM), (b) ATA2.0, (c) ATA4.0, (d) ATA6.0, and (e) ATA8.0. These panels show spatial distributions of the accumulated precipitation together with the time-average horizontal wind fields at the 500 hPa level, and their 72-h periods.

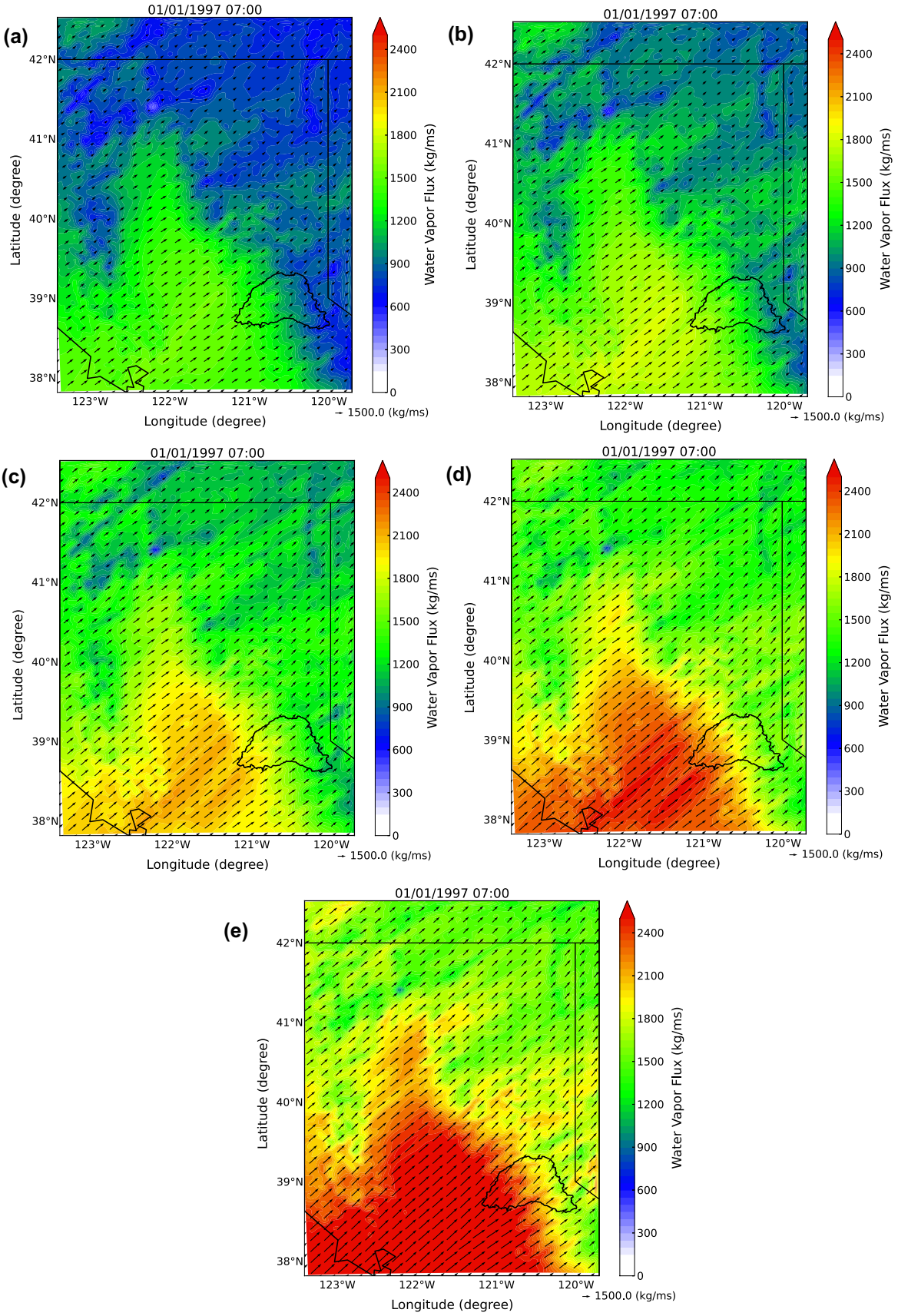

Fig. 8. Water vapor flux fields at 7:00 h on January 1, 1997 for (a) ATA0.0 (only ABCS + RHM), (b) ATA2.0, (c) ATA4.0, (d) ATA6.0, and (e) ATA8.0.

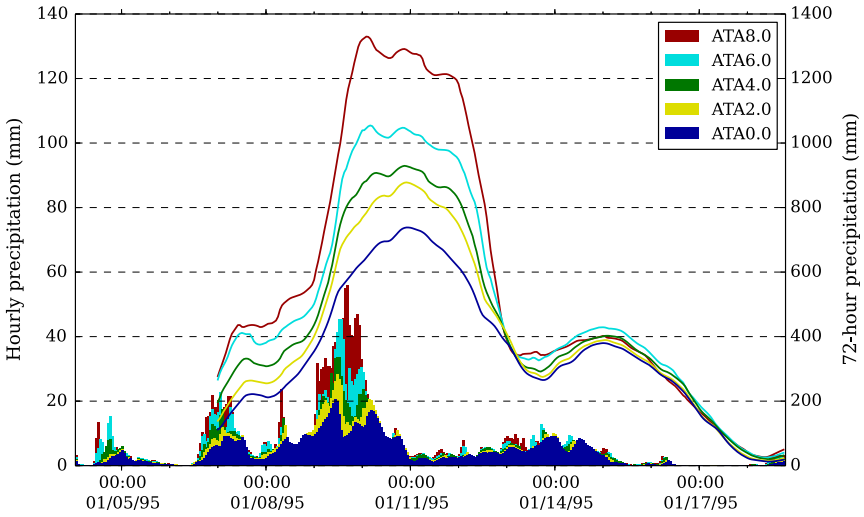

Fig. 9. Hourly basin-average precipitation (bar) and its 72-h moving summation (line) over the ARW for the A9501 storm event for ATA0.0 (only ABCS + RHM), ATA2.0, ATA4.0, ATA6.0, and ATA8.0.

of the hourly precipitation depth on January 7, 1995 is originally similar to the peak on January 14, 1995 during the A9501 storm event. However, the peak on January 14, 1995 is not amplified by the additional ATA method while the peak on January 7, 1995 is amplified. Fig. 12 shows water vapor flux fields before the peak on January 7, 1995. The water vapor flux of the high-moisture atmospheric flow is amplified by the additional ATA method, and the flow is directed toward the ARW. Meanwhile, water vapor flux fields before the first peak on January 14, 1995 are shown in Fig. 13. Although the water vapor flux of the high-moisture atmospheric flow before the first peak on January 14, 1995 is also amplified by the additional ATA method, the high-moisture atmospheric flow is not directed toward the ARW, but further north. Consequently, the additional ATA method magnifies the peak of the basin-average precipitation on January 7, 1995, but not the peaks on January 14, 1995. These results indicate that wind direction of the storm system is an important factor in the amplification of the basin-average precipitation by the additional ATA method.

Air temperature rise on the boundaries of the outer model domain almost monotonously increases the basin-average precipitation over the ARW as in Fig. 5 although the magnitude of increase in the basin-average precipitation by the additional ATA method may depend on the width of the atmospheric river(s) during a severe storm event. This monotonous increase in the basin-average precipitation with air temperature rise may imply the absence of an upper bound with respect to air temperature rise. However, 8.0 °C in air temperature rise may already be too large to occur realistically. Although the numerical experiments in this section provide some insight into the relationship between severe precipitation and air temperature rise, it will be unrealistic to raise the air temperature without considering its magnitude. It would be more realistic to consider a specific magnitude in air temperature rise from a source such as a future climate change assessment study, as investigated in the next section.

5.2. MP estimation under changing climate

The maximum 72-h basin-average precipitation over the ARW for the cases of ATA0.0 (ABCS + RHM), ATA1.36, and ATA3.16 for the 61 selected storm events is shown in Fig. 14. The maximum 72-h basin-average precipitation gradually increases for most of the storm events with the air temperature rise on the boundaries of the outer domain. On average, ATA1.36 and ATA3.16 (in addition to the ABCS + RHM) increase the maximum 72-h basin-average precipitation by 9.0% and by 20.3%, respectively. The largest rates of increase by ATA1.36 and ATA 3.16 are 16.2% for the A7803 storm event and 40.9% for the A7311 storm event, respectively. For relatively small storm events, the basin-average precipitation is hardly amplified by the additional ATA method although the maximum 72-h basin-average precipitation has decreased by ATA1.36 and ATA3.16 only for the A6801 storm event. On the other hand, no clear correlation was found in the maximum 72-h basin-average precipitation over the ARW between ATA0.0 (ABCS + RHM) and ATA1.36 or ATA3.16 (additional temperature rises over ABCS + RHM). While a monotonous increase with air temperature rise was found in the basin-average precipitation for each storm event similar to the A9501 and the A9701a storm events, the magnitude of increase in the basin-average precipitation by the additional ATA method is different among different storm events. These results imply the complexity of atmospheric processes that cause precipitation over a targeted watershed.

Consequently, from the addition of ATA to ABCS + RHM methods, the A9501 storm event was found to be the storm event with the largest basin-average precipitation depth for both of the cases ATA1.36 and ATA3.16. The MP estimates for this storm for the 72-h basin-average precipitation over the ARW by ATA1.36 and ATA3.16 are 846 mm and 940 mm, respectively. The historical largest value for the 72-h basin-average precipitation and the MP estimate by the ABCS + RHM method (ATA0.0) were 423 mm and 738 mm, respectively, over the ARW (Ishida et al., 2015a, 2015b). The MP estimates by ATA1.36 and ATA3.16 are respectively 100.0% and 122.2% larger than the historical largest value, and then respectively 14.6% and 27.3% larger than the MP estimate by the ABCS + RHM method (ATA0.0). The results of MP estimation by ATA1.36 and ATA3.16 are assumed to be the MP estimates for water years 2055 and 2099, respectively, under changing climate. In other words, the results by ATA1.36 and ATA3.16 indicate that the MP estimate will increase respectively by 14.6% and 27.3% in the middle and at the end of the 21st century, compared to the estimate under the historical climate conditions.

U.S. Army Corps of Engineers (2005) provides a precipitation frequency curve for the 72-h basin-average precipitation over the ARW. Whereas the MP estimate under the historical conditions corresponds to precipitation with approximately 35,000-year return period, the MP estimate for the end of the 21st century corresponds to precipitation with much more than 100,000 years of

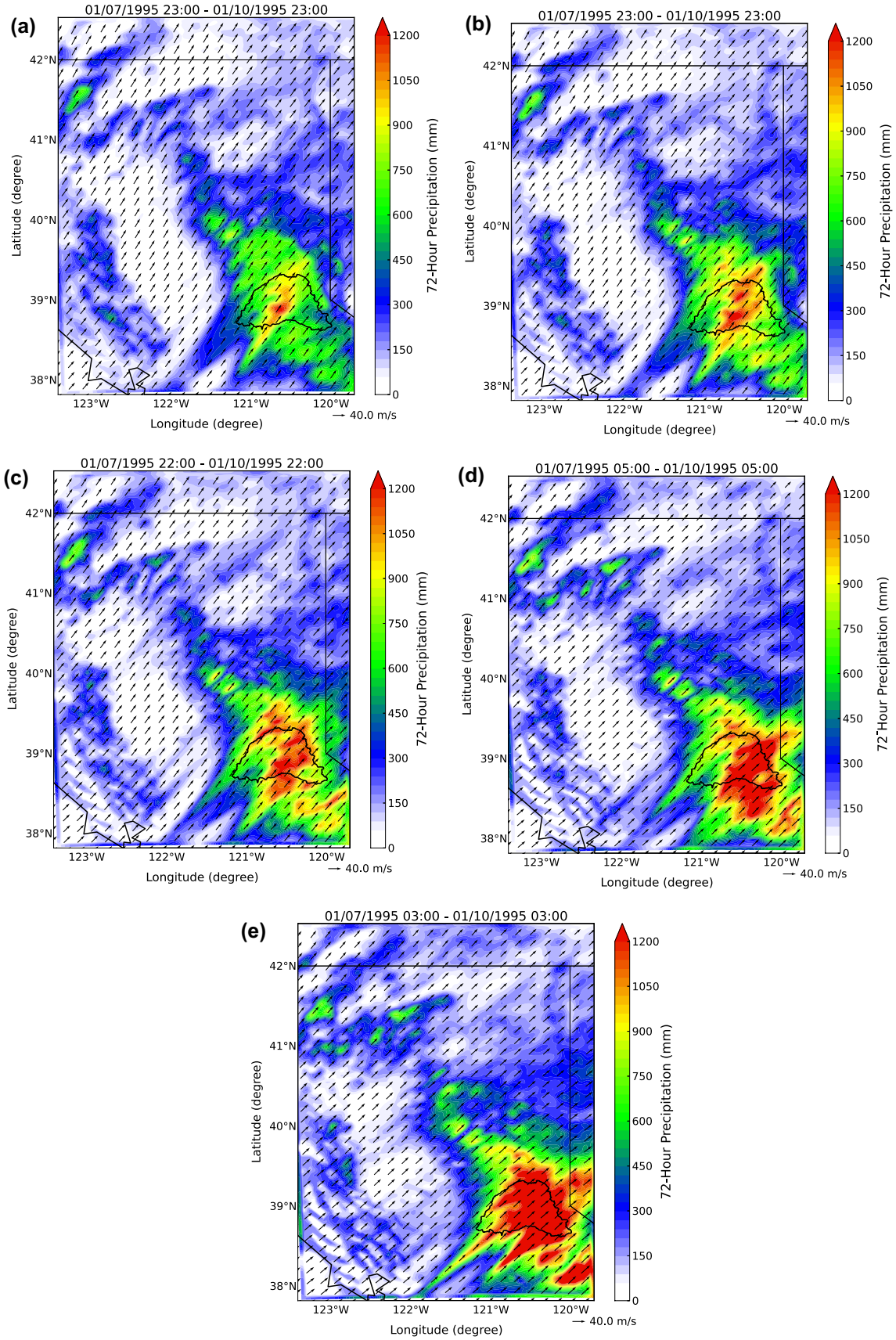

Fig. 10. 72-h precipitation depth for the A9501 storm event by (a) ATA0.0 (only ABCS + RHM), (b) ATA2.0, (c) ATA4.0, (d) ATA6.0, and (e) ATA8.0. These panels show spatial distributions of the accumulated precipitation together with the time-average horizontal wind fields at the 500 hPa level, and their 72-h periods.

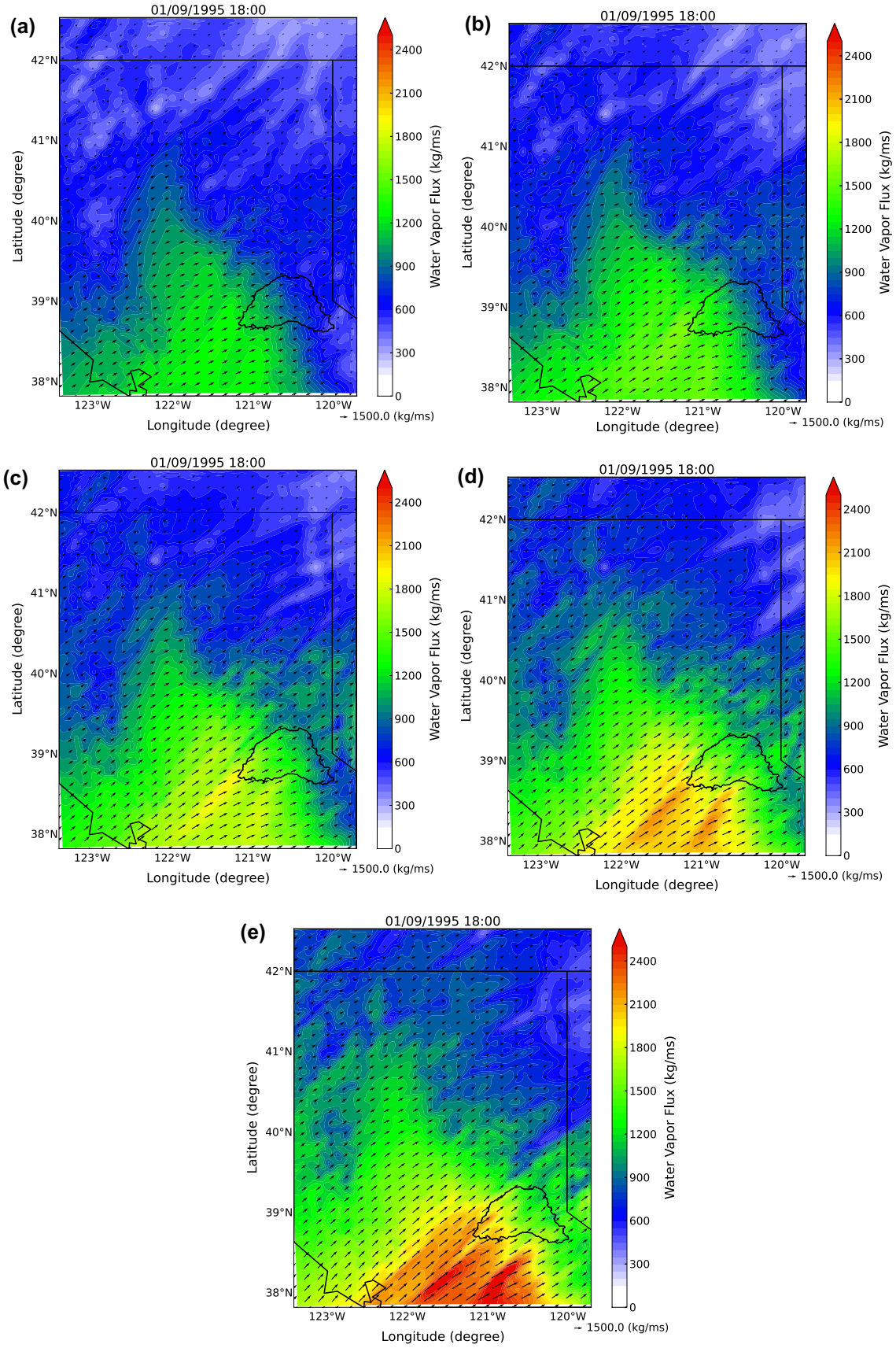

Fig. 11. Water vapor flux fields at 18:00 h on January 9, 1995 for (a) ATA0.0 (only ABCS + RHM), (b) ATA2.0, (c) ATA4.0, (d) ATA6.0, and (e) ATA8.0.

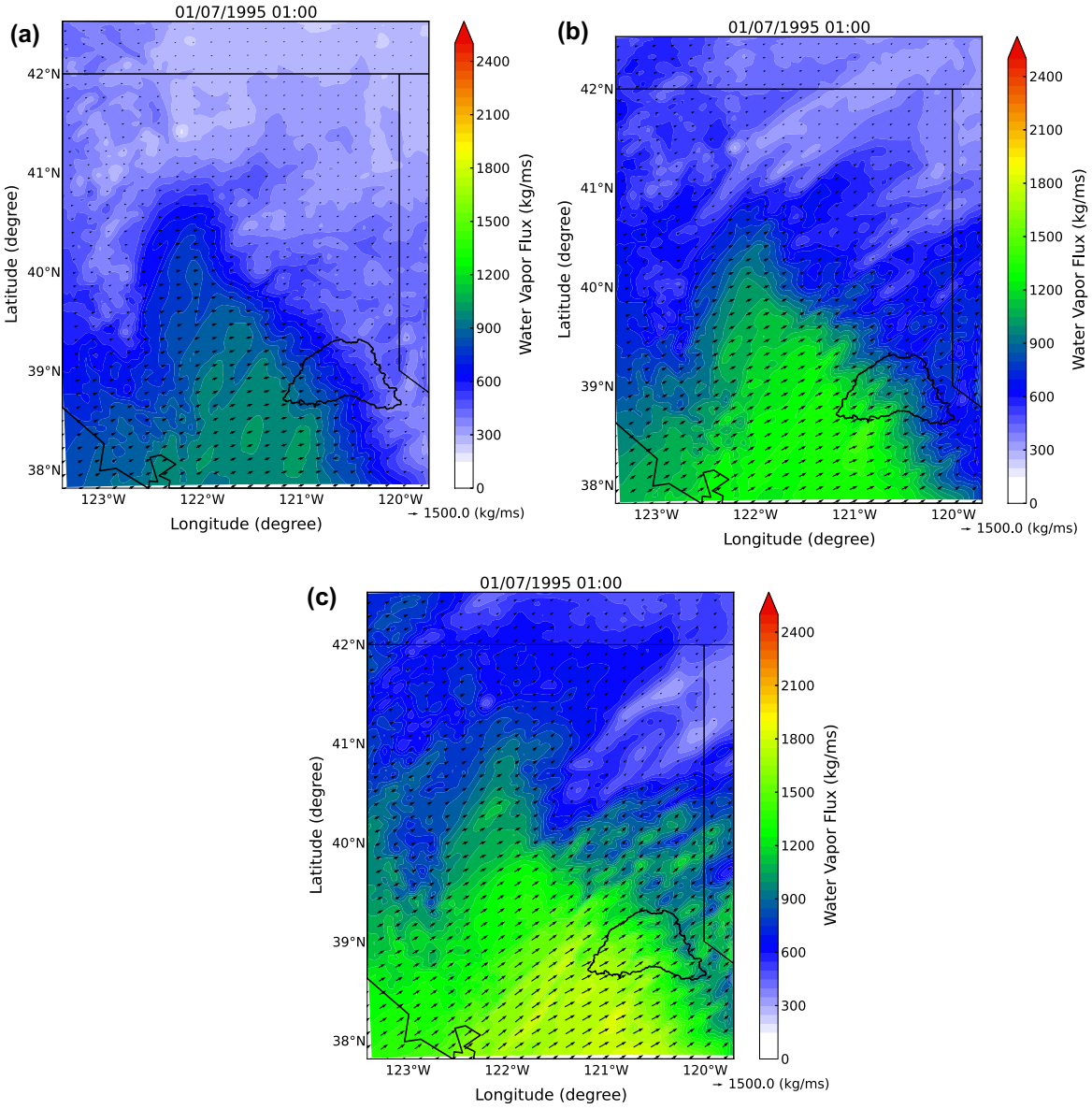

Fig. 12. Water vapor flux fields at 1:00 h on January 7, 1995 for (a) ATA0.0 (only ABCS + RHM), (b) ATA4.0, and (c) ATA8.0.

return period. Although the magnitudes of air temperature rise taken in this study for the future conditions may be arguable, it is highly likely that the ongoing global change in the climate may amplify the MP estimate over the ARW in the future.

6. Summary and conclusions

The Air Temperature Adjustment (ATA) method, as an additional procedure to Atmospheric Boundary Condition Shifting (ABCS) and Relative Humidity Maximization (RHM) procedures, was developed in this study for maximizing the basin average precipitation for a specified duration. Within this framework, the impact of air temperature on the MP estimate through change in moisture holding capacity of air was investigated over the ARW in Northern California, the United States as the target watershed. For this investigation, two types of numerical experiments were conducted by the ATA method. First, the air temperature on the entire lateral boundaries of the outer model domain was gradually increased from 0.0 °C to 8.0 °C by 0.5 °C increments for the A9701a and the A9501 storm events by the ATA method in addition to the ABCS + RHM method in order to investigate the sensitivity of the maximum 72-h basin-average precipitation over the ARW to air temperature rise uniformly at the entire model lateral boundaries. In this investigation, a monotonous increase was found in the maximum 72-h basin-average precipitation over the ARW with air temperature rise uniformly at the model boundaries for both of the storm events. Secondly, specific magnitudes of air temperature rise that represent future climate conditions during the 21st century were obtained from a climate change assessment study. The air temperature was increased uniformly by these specific magnitudes on the model boundaries by the ATA method in addition to the ABCS + RHM method to investigate the impact of air temperature on the MP estimate over the ARW under changing climate. The results in this second investigation indicate that future climate conditions may amplify the MP estimates that are based on historical conditions. The MP estimate may increase over the ARW by 14.6% in water year 2055 and by 27.3% in water year 2099 compared to the historical MP estimate.

The two types of numerical experiments that were performed in this study on the impact of air temperature on the MP estimate,

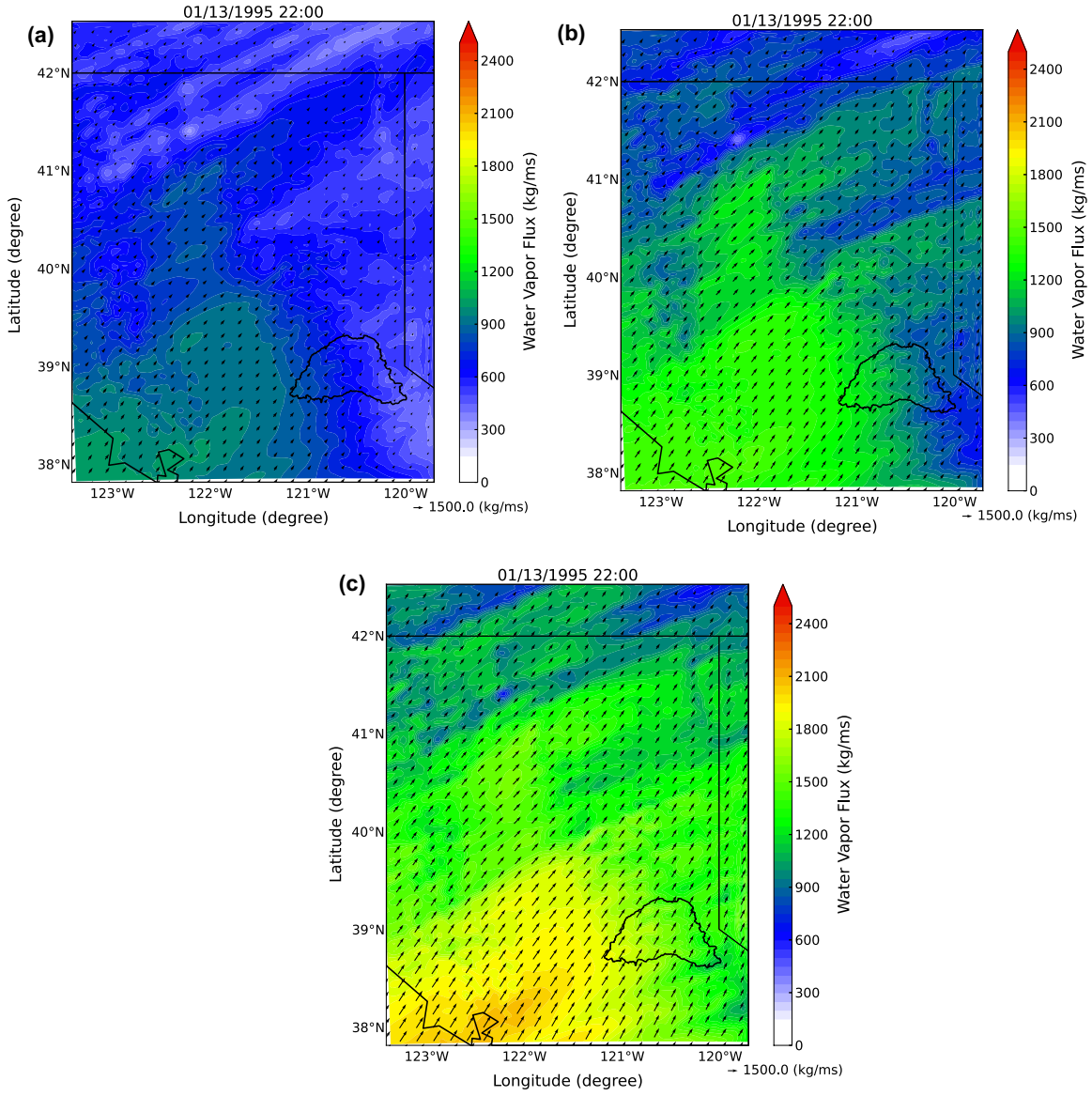

Fig. 13. Water vapor flux fields at 22:00 h on January 13, 1995 for (a) ATA0.0 (only ABCS + RHM), (b) ATA4.0, and (c) ATA8.0.

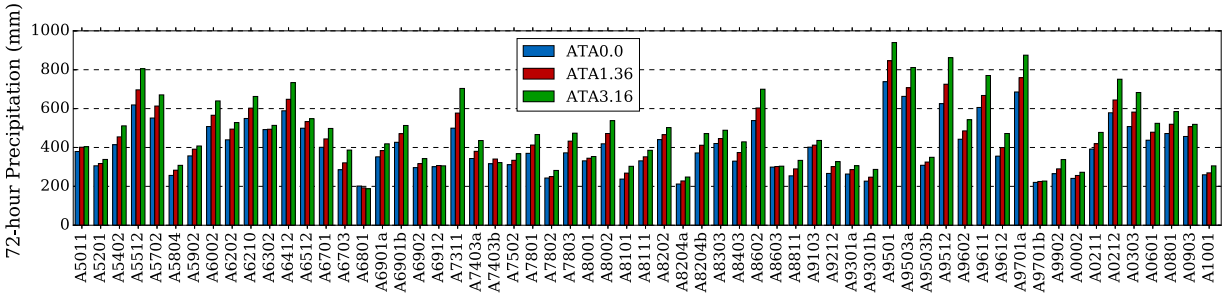

Fig. 14. Amplified maximum 72-h basin-average precipitation over the ARW for the 61 selected storm events for ATA0.0 (only ABCS + RHM), ATA1.36, and ATA3.16.

demonstrate the complexity of atmospheric systems that cause precipitation over a targeted watershed. The increase in the magnitude of the basin-average precipitation with air temperature rise uniformly on the model boundaries varies among hourly precipitation peaks within a storm event, depending on the direction of high-moisture atmospheric flow. The magnitude of increase in the basin-average precipitation also depends on each storm event although each storm event shows a monotonous increase in the basin-average precipitation with air temperature rise.

Air temperature is an important factor in the formation of severe precipitation. The results in this study show a high sensitivity of the MP estimate to air temperature rise. Meanwhile, the numerical simulation results of this study imply that the air temperature rise under saturated air moisture conditions may be able to

increase precipitation with no upper bound. As such, the magnitude of air temperature rise would be a key issue for the MP estimation, especially under future climate change conditions. Although in this study the magnitude of air temperature rise under future climate change conditions was obtained from a climate change assessment study, the magnitude of temperature rise should be estimated based on careful investigations and discussions in order to keep the MP estimate realistic. On the other hand, besides the air temperature, other atmospheric variables may also affect the precipitation depth although this study focused on the impact of air temperature (in addition to ABCS and RHM approaches) on the MP estimation through change in moisture holding capacity of air. Physical mechanisms to cause severe precipitation are very complicated. Therefore, it may be prudent to conduct the MP estimations within the framework of downscaled global circulation model future climate projections, especially in order to account for the impacts of air temperature, sea surface temperature, and other variables on the initiation and evolution of high-moisture atmospheric flows like ARs under changing climate.

References

Abbs, D.J., 1999. A numerical modeling study to investigate the assumptions used in the calculation of probable maximum precipitation. Water Resour. Res. 35, 785. http://dx.doi.org/10.1029/1998WR900013.

Casas, M.C., Rodríguez, R., Prohom, M., Gázquez, A., Redaño, A., 2011. Estimation of the probable maximum precipitation in Barcelona (Spain). Int. J. Climatol. 31, 1322–1327. http://dx.doi.org/10.1002/joc.2149.

Corrigan, P., Fenn, D.D., Kluck, D.R., Vogel, J.L., 1999. Probable Maximum Precipitation for California. Hydrometeorological Reports No. 59. National Oceanic and Atmospheric Administration, Silver Spring, MD.

Dudhia, J., 1996. A Multi-layer Soil Temperature Model for MM5, Preprints, 6th PSU/NCAR Mesoscale Model Users' Workshop. NCAR, Boulder, CO, pp. 19–50.

Fernando, W.C.D.K., Wickramasuriya, S.S., 2011. The hydro-meteorological estimation of probable maximum precipitation under varying scenarios in Sri Lanka. Int. J. Climatol. 31, 668–676. http://dx.doi.org/10.1002/joc.2096.

Grell, G.A., Dudhia, J., Stauffer, D., 1994. A Description of the Fifth-generation Penn State/NCAR Mesoscale Model, MM5, Boulder, CO, pp. 121.

Hong, S.-Y., Pan, H.-L., 1996. Nonlocal boundary layer vertical diffusion in a medium-range forecast model. Mon. Weather Rev. 124, 2322–2339. http://dx.doi.org/10.1175/1520-0493(1996)124<2322:NBLVDI>2.0.CO;2.

Ishida, K. et al., 2015a. Physically based estimation of maximum precipitation over three watersheds in Northern California: atmospheric boundary condition shifting. J. Hydrol. Eng. 20, 04014052. http://dx.doi.org/10.1061/(ASCE)HE.1943-5584.0001026.

Ishida, K. et al., 2015b. Physically based estimation of maximum precipitation over three watersheds in Northern California: relative humidity maximization method. J. Hydrol. Eng. http://dx.doi.org/10.1061/(ASCE)HE.1943-5584.0001175. 04015014.

Jang, S. et al., 2012. Regional Climate Change of Atmospheric Components in Northern California by Dynamic Downscaling, World Environmental and Water Resources Congress 2012. American Society of Civil Engineers, Reston, VA, pp. 1949–1956.

Kain, J.S., Fritsch, J.M., 1993. Convective parameterization for mesoscale models: the Kain-Fritsch scheme. In: Emanuel, K.A., Raymond, D.J. (Eds.), The Representation of Cumulus Convection in Numerical Models. American Meteorological Society, Boston, pp. 165–170.

Kalnay, E. et al., 1996. The NCEP/NCAR 40-year reanalysis project. Bull. Am. Meteorol. Soc. 77, 437–471. http://dx.doi.org/10.1175/1520-0477(1996)077<0437:TNYRP>2.0.CO;2.

Kavvas, M.L., Kure, S., Chen, Z.Q., Ohara, N., Jang, S., 2013. WEHY-HCM for modeling interactive atmospheric-hydrologic processes at watershed scale. I: model description. J. Hydrol. Eng. 18, 1262–1271. http://dx.doi.org/10.1061/(ASCE)HE.1943-5584.0000724.

Kay, A.L., Jones, R.G., Reynard, N.S., 2006. RCM rainfall for UK flood frequency estimation. II. Climate change results. J. Hydrol. 318, 163–172. http://dx.doi.org/10.1016/j.jhydrol.2005.06.013.

Kulkarni, B.D., Nandargi, S., Mulye, S.S., 2010. Zonal estimation of probable maximum precipitation rain depths over the Krishna basin in peninsular India. Hydrol. Sci. J. 55, 93–103. http://dx.doi.org/10.1080/02626660903529015.

Kunkel, K.E. et al., 2013. Probable maximum precipitation (PMP) and climate change. Geophys. Res. Lett. 40. http://dx.doi.org/10.1002/grl.50334.

Kure, S., Jang, S., Ohara, N., Kavvas, M.L., Chen, Z.Q., 2013. WEHY-HCM for modeling interactive atmospheric-hydrologic processes at watershed scale. II: model application to ungauged and sparsely gauged watersheds. J. Hydrol. Eng. 18, 1272–1281. http://dx.doi.org/10.1061/(ASCE)HE.1943-5584.0000701.

Markus, M., Wuebbles, D.J., Liang, X.-Z., Hayhoe, K., Kristovich, D.A.R., 2011. Diagnostic analysis of future climate scenarios applied to urban flooding in the Chicago metropolitan area. Clim. Change 111, 879–902. http://dx.doi.org/10.1007/s10584-011-0172-z.

National Center for Atmospheric Research (NCAR), 2005. PSU/NCAR Mesoscale Modeling System Tutorial Class Notes and User's Guide: MM5 Modeling System Version 3, Boulder, CO, pp. 8–13.

Ohara, N. et al., 2011. Physically based estimation of maximum precipitation over American River Watershed, California. J. Hydrol. Eng. 16, 351–361. http://dx.doi.org/10.1061/(ASCE)HE.1943-5584.0000324.

Papalexiou, S.M., Koutsoyiannis, D., 2006. A probabilistic approach to the concept of Probable Maximum Precipitation. Adv. Geosci. 7, 51–54. http://dx.doi.org/10.5194/adgeo-7-51-2006.

Reisner, J., Rasmussen, R.M., Bruintjes, R.T., 1998. Explicit forecasting of supercooled liquid water in winter storms using the MM5 mesoscale model. Q. J. R. Meteorol. Soc. 124, 1071–1107. http://dx.doi.org/10.1002/qj.49712454804.

Stallings, E.A., Cudworth, A.G., Hansen, E.M., Styner, W.A., 1986. Evolution of PMP cooperative studies. J. Water Resour. Plan. Manage. 112, 516–526. http://dx.doi.org/10.1061/(ASCE)0733-9496(1986)112:4(516).

Trinh, T. et al., 2016. New methodology to develop future flood frequency under changing climate by means of physically based numerical atmospheric-hydrologic modeling. J. Hydrol. Eng. 21 (4). http://dx.doi.org/10.1061/(ASCE)HE.1943-5584.0001331. 04016001.

U.S. Army Corps of Engineers, 2005. Stochastic Modeling of Extreme Floods on the American River at Folsom Dam: Flood-Frequency Curve Extension, Davis, California, pp. 46.

U.S. Weather Bureau, 1961. Interim Report-Probable Maximum Precipitation in California. Hydrometeorological Reports No. 36. U.S. Department of Commerce, Washington, D.C..

U.S. Weather Bureau, 1966. Interim Report-Probable Maximum Precipitation in California. Hydrometeorological Reports No. 43. U.S. Department of Commerce, Washington, D.C.

World Meteorological Organization (WMO), 1986. Manual for Estimation of Probable Maximum Precipitation, Geneva.

Yoshitani, J., Chen, Z.Q., Kavvas, M.L., Fukami, K., 2009. Atmospheric model-based streamflow forecasting at small, mountainous watersheds by a distributed hydrologic model: application to a watershed in Japan. J. Hydrol. Eng. 14, 1107–1118. http://dx.doi.org/10.1061/(ASCE)HE.1943-5584.0000111.

Zhan, D., Zhou, J., 1984. Recent developments on the probable maximum precipitation (PMP) estimation in China. J. Hydrol. 68, 285–293. http://dx.doi.org/10.1016/0022-1694(84)90216-6.